1

Modeling and Simulation of Multiphase Machines in the Matlab/Simulink Environment

Alberto Tessarolo
University of Trieste
Italy

1. Introduction

Multiphase machines are AC machines characterized by a stator winding composed of a generic number n of phases. In today's electric drive and power generation technology, multiphase machines play an important role for the benefits they bring compared to traditional three-phase ones (Levi, 2008; Levi et al., 2007). Such benefits have been widely highlighted by existing literature (Levi et al., 2007) and are mainly related to: an increased fault tolerance; higher power ratings achieved through power segmentation; enhanced performance in terms of efficiency and torque ripple.

The use of multiphase machines is spreading both in small-power safety-critical applications as well as in very high-power industrial drives (Tessarolo et al., 2010), in electric-propulsion drives (Castellan et al., 2007) and power generation systems (Sulligoi et al., 2010).

Regardless of whether they are used as motors or generators, multiphase electrical machines are almost always connected to power electronics systems (inverters for motors, rectifiers for generators), which interface them to the electric grid (Sulligoi et al., 2010; Castellan et al. 2008). Therefore, if the dynamic behaviour of a multiphase machine is to be predicted through simulations in the design and development stage, it is essential to do this by means of system-level simulations, where not only the electric machine is included, but also the power electronics and control systems that interact with it. Such a system-level simulation approach makes it difficult to use Finite-Element (FE) methods due to the complexity of the domain to be modelled and to the well-known computational heaviness of time-stepping FE simulations. Conversely, lumped-parameter models, to be implemented in the Matlab/Simulink environment, may provide designers with a powerful mean of analysis and investigation, provided that all the system components to be studied are modelled with an adequate level of accuracy and completeness.

As concerns power electronics systems usually interfaced to multiphase machines, whether operating as motors or generators, the Matlab/Simulink environment offers wide and complete libraries where the designer can find reliable pre-defined blocks (for electronic switches, snubbers, diodes, etc.) to be used in building the application-related apparatus models. The same pertains to control and regulation blocks, which can be built up directly based on their transfer functions and logics.

A possible criticality can be encountered when it comes to build the multiphase machine model. In fact, no predefined blocks are presently available in the Matlab/Simulink environment for this purpose. On the other side, building a dedicated user-defined machine

model for any specific multiphase arrangement may require a non-trivial work due to the wide variety of multiphase schemes (in terms of phase number and distribution) and due to the several different modelling approaches which can be derived from the current literature on the subject (Levi et al., 2007).

Based on the above premises, this Chapter aims at providing Matlab/Simulink users, interested in simulating electromechanical systems where multiphase machines are involved, with some general modelling and implementation strategies which enable them to treat all the multiphase machine schemes of practical interest in a unified manner.

The Chapter is organized so as to sequentially cover the topics listed below:

- Qualitative description of the various stator multiphase arrangements for multiphase machines.
- Introduction of Vector-Space Decomposition as a method for a unified treatment of the mentioned multiphase schemes.
- Implementation of the VSD-based model in the Matlab-Simulink environment.
- Application examples.

2. Variety, modelling and representation of multiphase winding schemes

There is a large variety of multiphase machines depending on:

1. The number of phases n constituting the stator winding;
2. The way in which the n phases are physically arranged;
3. The kind of rotor (which may be of squired-cage, permanent-magnet, reluctance, assisted-reluctance type as well as in ordinary three-phase machines).

As concerns phase arrangement, for instance, the n phases may be distributed symmetrically around the stator circumference with a phase shift of $360/n$ electrical degrees, as it happens in five-phase (Pereira et al., 2006) and seven-phase (Figueroa et al., 2006) symmetrical machines (Fig. 1a).

Otherwise, the n phases (with n necessarily being an integer multiple of 3) may be grouped into N three-phase sets, displaced by $60/N$ electrical degrees apart: this is the case of the so called split-phase winding configurations (Levi et al., 2007; Tessarolo et al., 2010) (Fig. 1b).

Finally, more complicated solutions can be also implemented, such as in the propulsion motor described by Terrein et al., 2004, where n=15 stator phases are grouped into three five-phase sets.

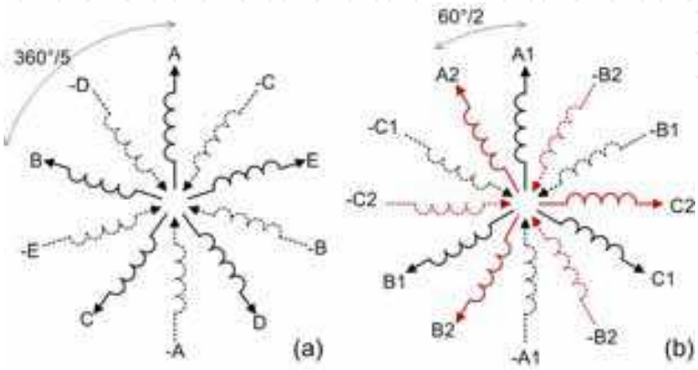

Fig. 1. Examples of multiphase winding schemes: (a) symmetrical 5-phase; (b) split-phase double-star

2.1 Graphical representation convention

The graphical representation of the winding scheme used in Fig. 1 is quite conventional and widespread. However, for the sake of clarity it can be better understood referring to Fig. 2 and Fig. 3, where such graphical representation is shown aside the physical phase arrangement in the case of a concentrated winding machine (the same pertains to distributed windings, of course). It can be seen that each coil group of the phase is represented by an arrow pointing in the direction of the magnetic field which would originate if the coil group carried a positive current. Coil groups shifted by 180 electrical degrees are represented by arrows of different line styles (solid and dashed).

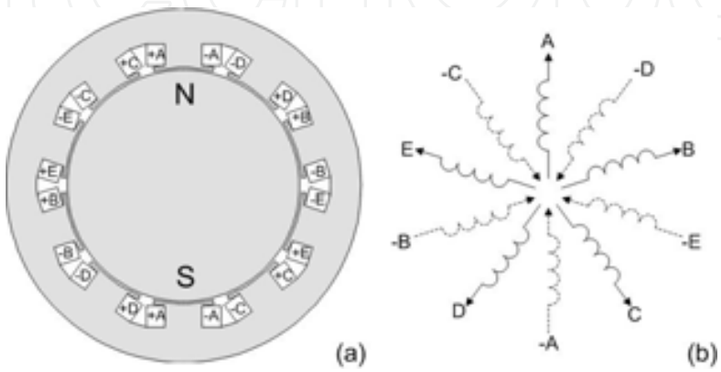

Fig. 2. Example of a two-pole 5-phase electric machine where each phase has coil groups shifted by π electrical radians

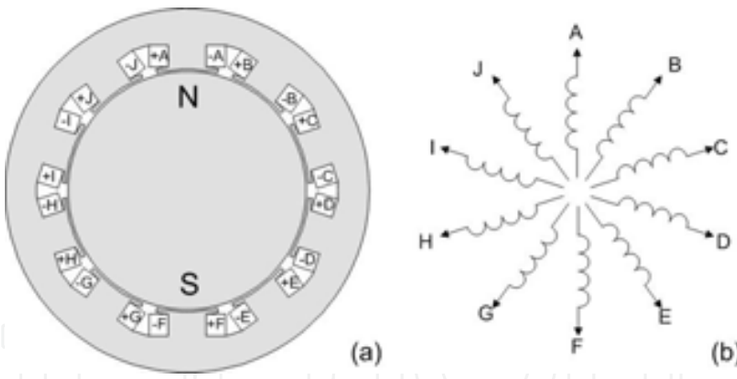

Fig. 3. Example of a two-pole 10-phase electric machine where each phase is not composed of coil groups shifted by π electrical radians. (a) Physical winding topology; (b) conventional winding representation

2.2 Modeling assumptions

In modelling the various types of multiphase machines, the following usual assumptions with be made in the rest of the Chapter:

1. Magnetic saturation is neglected, so inductances are assumed as constant.
2. It is assumed that the air-gap width of the machine can be modelled as a constant plus a sinusoidal function whose period equals a pole pitch.
3. All the *n* phases are geometrically identical except for their angular displacement, hence electrical machines with fractional slot windings are not covered.

4. Each phase is composed of identical coil groups (or phase belts) shifted by π electrical radians apart (as in the 5-phase example shown in Fig. 2); in other words, each phase has one coil group per pole. Conversely, such winding topologies as that shown in Fig. 3 (one phase belt per pole pair) and are not covered.

It is noticed that the assumption made in point 4 is not importantly restrictive, since such winding schemes as that shown in Fig. 3 are very rarely used in practice as they give rise to important even-order space harmonics in the air-gap (Klingshirn, 1983).

3. Multiphase machine modelling through Vector-Space Decomposition

The purpose of this Section is to propose a VSD method which applies to both symmetrical and asymmetrical *n*-phase winding schemes, for whatever integer n greater than 3. To do this, we propose that the VSD transformation should consist of two cascaded steps (Fig. 4):

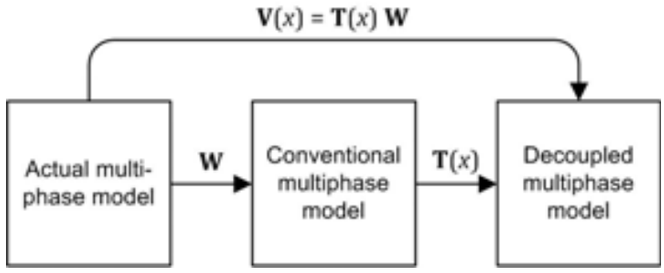

Fig. 4. Two-step transformation for the VSD of a generic multiphase model

1. The first is a merely geometrical transformation (**W**) capable of mapping the actual winding structure into a conventional one; the precise meaning of this "mapping" operation will be clarified next.
2. The second is a decoupling transformation [represented by matrix **T**(x) where x is the rotor position] to be applied to the conventional machine model. Such transformation is meant to project machine variables onto a set of mutually orthogonal subspaces.

The overall VSD transformation **V**(x)=**T**(x)**W** will then result from combining the two transformations. The advantage of this approach is that the properly called VSD theory can be developed only for the conventional multiphase model (thereby making abstraction of the particular phase arrangement of the actual machine), instead of tailoring VSD procedures on any particular multiphase winding topology that may occur in practice.

3.1 Selection of the conventional multiphase model

The question arises as to which multiphase model is the most suitable for being chosen as "conventional". A natural answer would be the symmetrical *n*-phase winding scheme with $2\pi/n$ phase progression, which is considered by Figueroa et al., 2006. With such a choice, the theory proposed in by Figueroa et al., 2006 could be in fact used to build the VSD transformation **V**(x). The problem which would occur with this choice, however, would be the lack of generality. In fact, there would be some *n*-phase schemes of practical importance which could not be mapped into an equivalent symmetrical winding with $2\pi/n$ phase progression through any transformation **W**. For instance, this would happen for any split-phase (multiple-star) windings composed of an even number of phases. The concept is illustrated in Fig. 5a-b; the figure shows how a triple-star winding can be certainly mapped

into a symmetrical 9-phase scheme with 2π/9 phase progression (through a transformation $\mathbf{W'}_{3\times3}$ mapping phase A1 into A, phase A2 into –F, phase A3 into B, etc.), while a dual-star winding (Fig. 5c) cannot be mapped into any 6-phase scheme with 2 π /6 phase progression, just because there does not exist a 6-phase scheme with 2 π /6 phase progression.

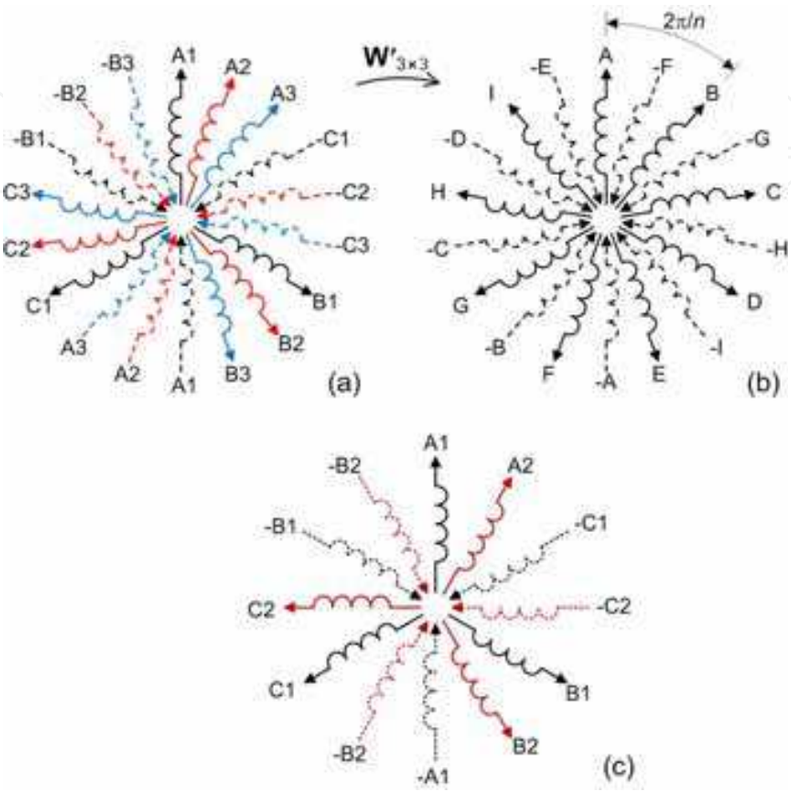

Fig. 5. Mapping of a triple-star winding (a) into a symmetrical 9-phase scheme with 2π/9 phase progression (b); a dual-star winding (c) cannot be mapped into any symmetrical 6-phase scheme with 2π/6 phase progression

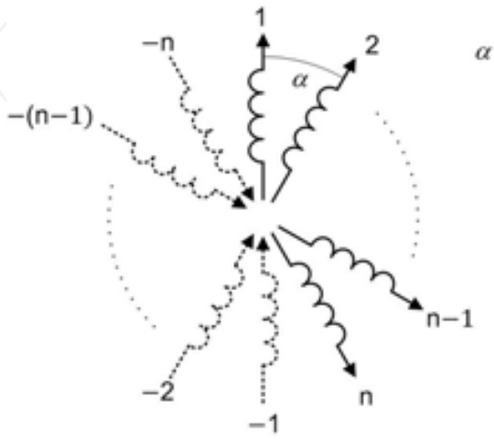

Fig. 6. Conventional arrangement for an n-phase winding

In order to overcome the above limitation, a different choice of the conventional multiphase scheme is made. The conventional *n*-phase winding arrangement selected for the purpose is shown in Fig. 6 and entails *n* phases numbered from 0 to n−1 and sequentially arranged over a pole span with a phase progression angle.

$$\alpha = \pi / n \tag{1}$$

With such a choice, any *n*-phase winding (whether symmetrical or asymmetrical, with even or odd phase count) can be mapped into a conventional n-phase arrangement such as that in Fig. 6 by means of a geometrical transformation **W**, built as detailed in the next Section.

3.2 Geometrical transformation into conventional winding scheme

By geometrical transformation we mean a sequence of phase permutations and reversals capable of reducing the actual winding scheme into an equivalent one having the conventional structure shown in Fig. 6. The principle is illustrated in Fig. 7 with the examples of a symmetrical 5-phase winding (a) and of an asymmetrical 6-phase (dual star) winding (c) to be mapped into their corresponding conventional arrangements respectively through transformations $\mathbf{W}_5$ and $\mathbf{W}_{2\times3}$.

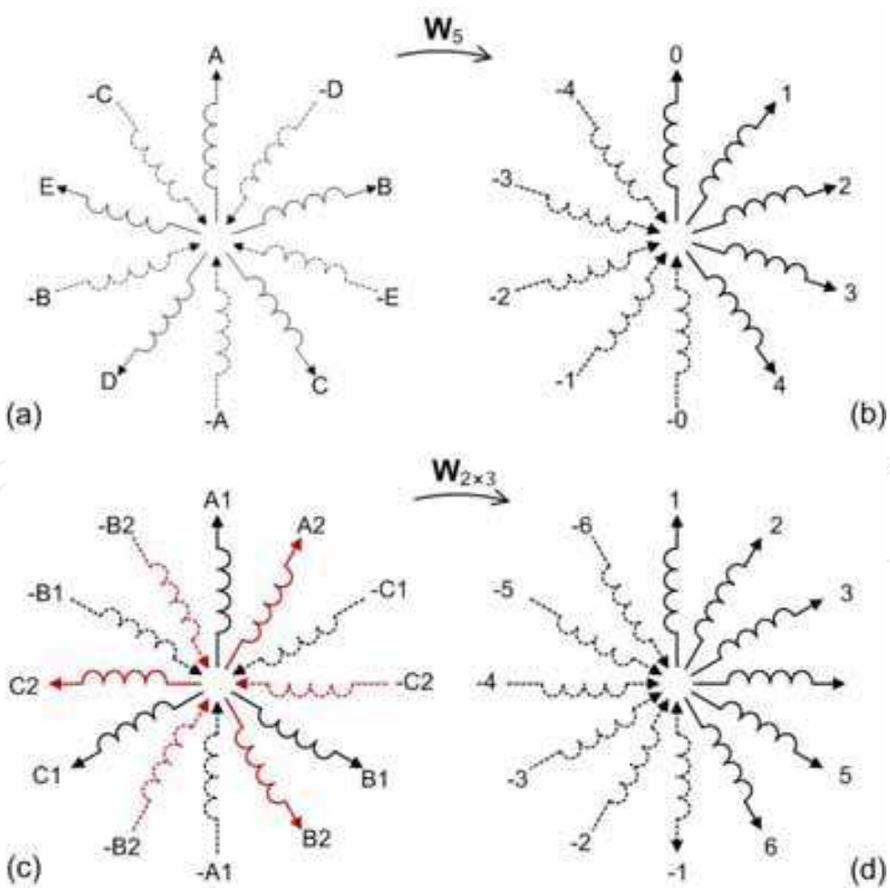

Fig. 7. Geometrical transformation into conventional phase arrangement

Let us suppose that the phase variables are arranged in vector form as per (2) and (3) respectively for the 5-phase and the dual star case and as per (4) for the conventional winding schemes:

$$\mathbf{y}_{A..E} = \begin{pmatrix} y_A & y_B & y_C & y_D & y_E \end{pmatrix}^t \tag{2}$$

$$\mathbf{y}_{2\times ABC} = \begin{pmatrix} y_{A1} & y_{A2} & y_{B1} & y_{B2} & y_{C1} & y_{C2} \end{pmatrix}^t \tag{3}$$

$$\mathbf{y}_n = \begin{pmatrix} y_0 & y_1 & y_2 & \cdots & y_{n-1} \end{pmatrix}^t \tag{4}$$

where y indicates a generic phase variable, such as a current, voltage or flux linkage and superscript t indicates transposition. It can be easily seen that the following relationships must hold for the windings (a), (c) to be respectively equivalent to windings (b), (d) in Fig. 7:

$$\mathbf{y}_5 = \mathbf{W}_5 \mathbf{y}_{A..E}, \quad \mathbf{W}_5 = \begin{pmatrix} 1 & 0 & 0 & 0 & 0 \\ 0 & 0 & 0 & -1 & 0 \\ 0 & 1 & 0 & 0 & 0 \\ 0 & 0 & 0 & 0 & -1 \\ 0 & 0 & 1 & 0 & 0 \end{pmatrix} \tag{5}$$

$$\mathbf{y}_6 = \mathbf{W}_{2\times 3} \mathbf{y}_{2\times ABC}, \quad \mathbf{W}_{2\times 3} = \begin{pmatrix} 1 & 0 & 0 & 0 & 0 & 0 \\ 0 & 0 & 0 & 1 & 0 & 0 \\ 0 & 0 & -1 & 0 & 0 & 0 \\ 0 & 0 & 0 & 0 & 0 & -1 \\ 0 & 1 & 0 & 0 & 0 & 0 \\ 0 & 0 & 0 & 0 & 1 & 0 \end{pmatrix} \tag{6}$$

3.2.1 General transformation for symmetrical *n*-phase configurations

Let us now consider the general case of a symmetrical n-phase winding with $2\pi/n$ phase progression (see Fig. 1a and Fig. 5b as examples); it can be mapped into a conventional phase arrangement through the geometrical transformation $\mathbf{W}_n$ defined as:

$$\left\{\mathbf{W}_n\right\}_{i,j} = \begin{cases} 1 & \text{if } 2j - i = 0 \\ -1 & \text{if } \left|2j - i\right| = n \\ 0 & \text{otherwise} \end{cases} \qquad i, j = 0, ..., n-1; \tag{7}$$

The formal proof of (7) is omitted for the sake of brevity as the formula can be easily checked on a case-by-case basis.

3.2.2 General transformation for asymmetrical (split-phase) configurations

Let us consider the general case of an asymmetrical (or split-phase) winding composed of N m-phase stars shifted by $2\pi/(mN)$ stars (Fig. 5a shows an example with m=3 and N=3, Fig. 1b with m=3 and N=2). Such a winding can be mapped into a conventional mN-phase arrangement through the geometrical transformation given by:

$$\left\{\mathbf{W}_{N\times m}\right\}_{i,j}=\begin{cases}1 & \text{if } i-\text{trunc}\left(j/m\right)-2N\,\text{mod}(j,m)=0\\ -1 & \text{if } \left|i-\text{trunc}\left(j/m\right)-2N\,\text{mod}(j,m)\right|=mN \\ 0 & \text{otherwise}\end{cases} \qquad i,j=0,...,mN-1\,; \quad (8)$$

The formula can be easily checked to hold on a case-by-case basis.

3.3 Machine model in conventional multiphase variables

In the previous Section it has been shown how any multiphase scheme can be mapped into an equivalent one having a "conventional" phase arrangement and the suitable variable transformation matrices to be applied for this purpose have been presented. Therefore, it is not restrictive to suppose, in the following, that stator phases are distributed according to the conventional scheme. Hereinafter we shall present the form that the machine model equations take in this case.

The stator voltage equation in matrix form is given by:

$$\mathbf{v}_s=\mathbf{R}_s\mathbf{i}_s+\frac{d}{dt}\boldsymbol{\varphi}_s+\mathbf{e}_s \tag{9}$$

where phase variables are (superscript t denotes transposition):

$$\mathbf{v}_s=\begin{pmatrix}v_0 & v_1 & \cdots & v_{n-2} & v_{n-1}\end{pmatrix}^t \tag{10}$$

$$\mathbf{i}_s=\begin{pmatrix}i_0 & i_1 & \cdots & i_{n-2} & i_{n-1}\end{pmatrix}^t \tag{11}$$

$$\boldsymbol{\varphi}_s=\begin{pmatrix}\varphi_0 & \varphi_1 & \cdots & \varphi_{n-2} & \varphi_{n-1}\end{pmatrix}^t \tag{12}$$

$$\mathbf{e}_s=\begin{pmatrix}e_0 & e_1 & \cdots & e_{n-2} & e_{n-1}\end{pmatrix}^t \tag{13}$$

The symbol x_k , with $x \in \{v, i, \varphi, e\}$ and $k \in \{0, 1,\ldots, n-1\}$ represents the k^{th} phase voltage (v), current (i), flux linkage (φ) or e.m.f. due to the rotor (e). The resistance matrix $\mathbf{R}$ is the $n\times n$ diagonal matrix having all its diagonal elements equal to phase resistance r:

$$\mathbf{R}_s=\begin{pmatrix}r & 0 & & 0\\ 0 & r & & 0\\ & & \ddots & \\ 0 & 0 & & r\end{pmatrix} \tag{14}$$

Phase flux linkage and current vectors are linked by the stator inductance matrix $\mathbf{L}$ which, for salient-pole machines, is a function of the rotor position x.

$$\boldsymbol{\varphi}_s=\mathbf{L}_s\left(x\right)\mathbf{i}_s \tag{15}$$

The stator inductance matrix is assumed to be composed of a leakage inductance term $\mathbf{L}_s^{(l)}$, not dependent on rotor position, and of an air-gap inductance term $\mathbf{L}_s^{(ag)}\left(x\right)$:

$$\mathbf{L}_s(x) = \mathbf{L}_s^{(l)} + \mathbf{L}_s^{(ag)}(x) \tag{16}$$

Substitution of (16) into (9) gives:

$$\mathbf{v}_s = \mathbf{R}_s\mathbf{i}_s + \frac{d}{dt}\left(\mathbf{L}_s\mathbf{i}_s\right) + \mathbf{e}_s = \mathbf{R}_s\mathbf{i}_s + \left(\frac{d}{dt}\mathbf{L}_s\right)\mathbf{i}_s + \mathbf{L}_s\frac{d}{dt}\mathbf{i}_s + \mathbf{e}_s \tag{17}$$

It is easy to show (Tessarolo, 2010) that the leakage inductance matrix has the following structure.

$$\mathbf{L}_s^{(l)} = \begin{pmatrix} \ell_0 & \ell_1 & \ell_2 & & -\ell_3 & -\ell_2 & -\ell_1 \\ \ell_1 & \ell_0 & \ell_1 & \cdots & -\ell_4 & -\ell_3 & -\ell_2 \\ \ell_2 & \ell_1 & \ell_0 & & -\ell_5 & -\ell_4 & -\ell_3 \\ & \vdots & & & & \vdots & \\ -\ell_3 & -\ell_4 & -\ell_5 & & \ell_0 & \ell_1 & \ell_2 \\ -\ell_2 & -\ell_3 & -\ell_4 & \cdots & \ell_1 & \ell_0 & \ell_1 \\ -\ell_1 & -\ell_2 & -\ell_3 & & \ell_2 & \ell_1 & \ell_0 \end{pmatrix} \tag{18}$$

Based on the assumptions listed in 2.2, the air-gap inductance matrix can be written as:

$$\mathbf{L}_s^{(ag)} = \frac{L_{md} + L_{mq}}{2}\mathbf{\Gamma}_1 + \frac{L_{md} - L_{mq}}{2}\left[\mathbf{\Gamma}_2\cos(2x) + \mathbf{\Gamma}_3\sin(2x)\right] \tag{19}$$

where:

$$\mathbf{\Gamma}_1 = \begin{pmatrix} 1 & \cos(\alpha) & \cos(2\alpha) & \cos(3\alpha) & \\ \cos(\alpha) & \cos(2\alpha) & \cos(3\alpha) & & \\ \cos(2\alpha) & \cos(3\alpha) & & & \\ \cos(3\alpha) & & \ddots & & \\ & & & & \end{pmatrix} \tag{20}$$

$$\mathbf{\Gamma}_2 = \begin{pmatrix} 1 & \cos(\alpha) & \cos(2\alpha) & \cos(3\alpha) & \\ \cos(\alpha) & 1 & \cos(\alpha) & \cos(2\alpha) & \\ \cos(2\alpha) & \cos(\alpha) & 1 & \cos(\alpha) & \\ \cos(3\alpha) & \cos(2\alpha) & \cos(\alpha) & 1 & \\ & & & & \ddots \end{pmatrix} \tag{21}$$

$$\mathbf{\Gamma}_3 = \begin{pmatrix} 1 & \sin(\alpha) & \sin(2\alpha) & \sin(3\alpha) & \\ \sin(\alpha) & 1 & \sin(\alpha) & \sin(2\alpha) & \\ \sin(2\alpha) & \sin(\alpha) & 1 & \sin(\alpha) & \\ \sin(3\alpha) & \sin(2\alpha) & \sin(\alpha) & 1 & \\ & & & & \ddots \end{pmatrix} \tag{22}$$

Equations (19)-(22) directly descend from the expression of the mutual inductance (due to air-gap flux) between two phases of indices “i” and “j” (Tessarolo et al., 2009):

$$\left[\mathbf{L}_{\mathrm{s}}^{(ag)}\right]_{i,j}=\frac{L_{md}+L_{mq}}{2}\cos\left[(i-j)\alpha\right]+\frac{L_{md}-L_{mq}}{2}\cos\left[2\left(x-\frac{i+j}{2}\alpha\right)\right] \tag{23}$$

3.4 VFD transformation matrix

The problem with the machine model expressed in multiphase variables is that stator model matrices are not constant in presence of rotor saliency ($L_{md} \neq L_{mq}$), as shown by (23). Furthermore, it would be desirable that model variables become constant during sinusoidal steady-state operation. Additionally, the model written as per 3.2 contains quite involved inductance matrix structure and is thereby little suitable for implementation. Finally, a simple expression for the machine torque cannot be derived from the model formulated as per 3.2.

Vector-Space Decomposition (VSD) is a modelling technique which enables one to significantly simplify the machine equations (Levi et al., 2007) and finally yields a model structure (including diagonal matrices) which is simple to implement numerically. VSD, as proposed in this Chapter, is based on using a variable transformation **T** which maps the conventional multiphase vector variables (10)-(13) into "orhtonormal" vector coordinates (denoted with subscript *dq* in the following) as per (24). Model matrices are accordingly transformed as per (25).

$$\mathbf{v}_{dq}=\mathbf{T}(x)\mathbf{v}_s,\ \mathbf{i}_{dq}=\mathbf{T}(x)\mathbf{i}_s,\ \boldsymbol{\varphi}_{dq}=\mathbf{T}(x)\boldsymbol{\varphi}_s,\ \mathbf{e}_{dq}=\mathbf{T}(x)\mathbf{e}_s \tag{24}$$

The transformation matrix **T**(x) proposed here to accomplish the VSD is given by:

$$\mathbf{T}(x)=\mathbf{P}(x)\mathbf{C} \tag{25}$$

where:

$$\mathbf{P}(x)=\left(\begin{array}{cc|cc|cc|c} \cos(\omega x) & \sin(\omega x) & 0 & 0 & 0 & 0 & \\ -\sin(\omega x) & \cos(\omega x) & 0 & 0 & 0 & 0 & \\ \hline 0 & 0 & \cos(3\omega x) & \sin(3\omega x) & 0 & 0 & \\ 0 & 0 & -\sin(3\omega x) & \cos(3\omega x) & 0 & 0 & \\ \hline 0 & 0 & 0 & 0 & \cos(5\omega x) & \sin(5\omega x) & \\ 0 & 0 & 0 & 0 & -\sin(5\omega x) & \cos(5\omega x) & \\ \hline & & & & & & \ddots \end{array}\right) \tag{26}$$

$$\mathbf{C}=\sqrt{\frac{2}{n}}\left(\begin{array}{ccccccc} 1 & \cos(\alpha) & \cos(2\alpha) & \cos(3\alpha) & \cdots & \cos\left[(n-1)\alpha\right] \\ 0 & \sin(\alpha) & \sin(2\alpha) & \sin(3\alpha) & \cdots & \sin\left[(n-1)\alpha\right] \\ \hline 1 & \cos(3\alpha) & \cos(6\alpha) & \cos(9\alpha) & \cdots & \cos\left[3(n-1)\alpha\right] \\ 0 & \sin(3\alpha) & \sin(6\alpha) & \sin(9\alpha) & \cdots & \sin\left[3(n-1)\alpha\right] \\ \hline 1 & \cos(5\alpha) & \cos(10\alpha) & \cos(15\alpha) & \cdots & \cos\left[5(n-1)\alpha\right] \\ 0 & \sin(5\alpha) & \sin(10\alpha) & \sin(10\alpha) & \cdots & \sin\left[5(n-1)\alpha\right] \\ \hline \vdots & \vdots & \vdots & \vdots & & \vdots \end{array}\right) \tag{27}$$

We notice that the proposed matrices do not coincide either with those used by Figueroa et al., 2006, or with those mentioned in Levi et al., 2007, but are specifically design to treat an *n*-phase machine with conventional multiphase arrangement (Tessarolo, 2009).

3.5 Machine model in transformed coordinates

In this Section, the transformation $\mathbf{T}(x)$ defined above will be applied to the model of the *n*-phase salient-pole machine whose model in conventional multiphase coordinates has been established in 3.2.

By applying transformation $\mathbf{T}(x)$ to model variables as per (24) and matrices (16) and (16) we obtain the transformed model matrices (marked by subscript *dq*) below:

$$\mathbf{R}_{dq} = \mathbf{T}(x)\mathbf{R}_s\mathbf{T}(x)^t = \mathbf{T}(x)\left(r\mathbf{I}\right)\mathbf{T}(x)^t = r\mathbf{T}(x)\mathbf{T}(x)^t = r\mathbf{I} = \mathbf{R}_s \tag{28}$$

$$\mathbf{L}_{dq} = \mathbf{L}_{dq}^{(l)} + \mathbf{L}_{dq}^{(ag)} = \mathbf{T}(x)\mathbf{L}_s(x)\mathbf{T}(x)^t = \mathbf{T}(x)\mathbf{L}_{dq}^{(l)}\mathbf{T}(x)^t + \mathbf{T}(x)\mathbf{L}_{dq}^{(l)}\mathbf{T}(x)^t \tag{29}$$

More precisely, the transformed leakage inductance matrix takes the diagonal form (Tessarolo, 2009):

$$\mathbf{L}_{dq}^{(l)} = \mathbf{T}(x)\mathbf{L}_{dq}^{(l)}\mathbf{T}(x)^t = \begin{pmatrix} \lambda_1 & 0 & 0 & 0 & 0 & 0 & \\ 0 & \lambda_1 & 0 & 0 & 0 & 0 & \\ 0 & 0 & \lambda_3 & 0 & 0 & 0 & \\ 0 & 0 & 0 & \lambda_3 & 0 & 0 & \ddots \\ 0 & 0 & 0 & 0 & \lambda_5 & 0 & \\ 0 & 0 & 0 & 0 & 0 & \lambda_5 & \\ & & & \ddots & & & \ddots \end{pmatrix} \tag{30}$$

where:

$$\lambda_h = \ell_0 + 2\sum_{k=0}^{n-1} \ell_k \cos\left(kh\alpha\right) \tag{31}$$

for h = 1, 3, 5, ... is the harmonic inductance of the machine of order h (Tessarolo, 2009).

The air-gap inductance matrix becomes:

$$\begin{aligned} \mathbf{L}_{dq}^{(ag)} &= \mathbf{T}(x)\mathbf{L}_{dq}^{(ag)}\mathbf{T}(x)^t = \frac{L_{md}+L_{mq}}{2}\mathbf{T}(x)\mathbf{\Gamma}_1\mathbf{T}(x)^t \\ &+ \frac{L_{md}-L_{mq}}{2}\left[\mathbf{T}(x)\mathbf{\Gamma}_2\mathbf{T}(x)^t\cos\left(2x\right) + \mathbf{T}(x)\mathbf{\Gamma}_3\mathbf{T}(x)^t\sin\left(2x\right)\right] \\ &= n\begin{pmatrix} L_{md} & 0 & 0 & 0 & \\ 0 & L_{mq} & 0 & 0 & \\ 0 & 0 & 0 & 0 & \\ 0 & 0 & 0 & 0 & \\ & & & & \ddots \end{pmatrix} \end{aligned} \tag{32}$$

The overall inductance matrix in transformed coordinates is then the diagonal matrix below:

$$\mathbf{L}_{dq} = \begin{pmatrix} nL_{md}+\lambda_1 & 0 & 0 & 0 & 0 & 0 & \\ 0 & nL_{md}+\lambda_1 & 0 & 0 & 0 & 0 & \\ 0 & 0 & \lambda_3 & 0 & 0 & 0 & \\ 0 & 0 & 0 & \lambda_3 & 0 & 0 & \ddots \\ 0 & 0 & 0 & 0 & \lambda_5 & 0 & \\ 0 & 0 & 0 & 0 & 0 & \lambda_5 & \\ & & & \ddots & & & \ddots \end{pmatrix} \tag{33}$$

Using (24), the relationship (15) between the flux linkage and current vectors becomes:

$$\boldsymbol{\varphi}_s = \mathbf{T}(x)^t \boldsymbol{\varphi}_{dq} = \mathbf{L}_s(x)\mathbf{T}(x)^t \mathbf{i}_{dq} \quad \Rightarrow \quad \boldsymbol{\varphi}_{dq} = \mathbf{T}(x)\mathbf{L}_s(x)\mathbf{T}(x)^t \mathbf{i}_{dq} \tag{34}$$

which, in virtue of (29), gives:

$$\boldsymbol{\varphi}_{dq} = \mathbf{L}_{dq}\mathbf{i}_{dq} \tag{35}$$

Using the above relationships, the stator voltage equation (9) becomes:

$$\begin{aligned} \mathbf{v}_s = \mathbf{T}(x)^t \mathbf{v}_{dq} &= \mathbf{R}_s \mathbf{T}(x)^t \mathbf{i}_{dq} + \frac{d}{dt}\left[\mathbf{T}(x)^t \boldsymbol{\varphi}_{dq}\right] + \mathbf{e}_s \\ &= \mathbf{R}_s \mathbf{T}(x)^t \mathbf{i}_{dq} + \frac{d}{dt}\left[\mathbf{T}(x)^t \mathbf{L}_{dq}\mathbf{i}_{dq}\right] + \mathbf{e}_s \\ &= \mathbf{R}_s \mathbf{T}(x)^t \mathbf{i}_{dq} + \left[\frac{d}{dt}\mathbf{T}(x)^t\right]\left[\mathbf{L}_{dq}\mathbf{i}_{dq}\right] + \mathbf{T}(x)^t \frac{d}{dt}\left[\mathbf{L}_{dq}\mathbf{i}_{dq}\right] + \mathbf{e}_s \\ &= \mathbf{R}_s \mathbf{T}(x)^t \mathbf{i}_{dq} + \left[\frac{d}{dt}\mathbf{T}(x)^t\right]\left[\mathbf{L}_{dq}\mathbf{i}_{dq}\right] + \mathbf{T}(x)^t \mathbf{L}_{dq}\frac{d}{dt}\mathbf{i}_{dq} + \mathbf{e}_s \end{aligned} \tag{36}$$

It is important to remark that in the last passage of (37), we have used the fact that L_{dq}, given by (34), is time-invariant, i.e.

$$\tfrac{d}{dt}\mathbf{L}_{dq} = \mathbf{0} \tag{37}$$

so that it is correct to write:

$$\tfrac{d}{dt}\left[\mathbf{L}_{dq}\mathbf{i}_{dq}\right] = \left[\tfrac{d}{dt}\mathbf{L}_{dq}\right]\mathbf{i}_{dq} + \mathbf{L}_{dq}\tfrac{d}{dt}\mathbf{i}_{dq} = \mathbf{L}_{dq}\tfrac{d}{dt}\mathbf{i}_{dq} \tag{38}$$

If we left-multiply (37) by $\mathbf{T}(x)$ we obtain:

$$\begin{aligned} \mathbf{T}(x)\mathbf{v}_s = \mathbf{v}_{dq} &= \mathbf{T}(x)\mathbf{R}_s\mathbf{T}(x)^t\mathbf{i}_{dq} + \mathbf{T}(x)\left[\frac{d}{dt}\mathbf{T}(x)^t\right]\mathbf{L}_{dq}\mathbf{i}_{dq} + \mathbf{L}_{dq}\frac{d}{dt}\mathbf{i}_{dq} + \mathbf{T}(x)\mathbf{e}_{dq} \\ &= \mathbf{R}_{dq}\mathbf{i}_{dq} + \mathbf{T}(x)\left[\frac{dx}{dt}\frac{d}{dx}\mathbf{T}(x)^t\right]\mathbf{L}_{dq}\mathbf{i}_{dq} + \mathbf{L}_{dq}\frac{d}{dt}\mathbf{i}_{dq} + \mathbf{e}_{dq} \\ &= \mathbf{R}_{dq}\mathbf{i}_{dq} + \omega\mathbf{T}(x)\left[\frac{d}{dx}\mathbf{T}(x)^t\right]\mathbf{L}_{dq}\mathbf{i}_{dq} + \mathbf{L}_{dq}\frac{d}{dt}\mathbf{i}_{dq} + \mathbf{e}_{dq} \end{aligned} \tag{39}$$

where the rotor speed in electrical radians per second has been introduced:

$$\omega = \frac{dx}{dt} \tag{40}$$

The product $\mathbf{T}(x)\left[\frac{d}{dx}\mathbf{T}(x)^t\right]$ in (40) can be expanded using (25) as follows:

$$\begin{aligned}\mathbf{T}(x)\left[\frac{d}{dx}\mathbf{T}(x)^t\right] &= \mathbf{P}(x)\mathbf{C}\left[\frac{d}{dx}\mathbf{C}^t\mathbf{P}(x)^t\right] = \mathbf{P}(x)\mathbf{C}\left\{\left(\frac{d}{dx}\mathbf{C}^t\right)\mathbf{P}(x)^t + \mathbf{C}^t\left[\frac{d}{dx}\mathbf{P}(x)^t\right]\right\} \\ &= \mathbf{P}(x)\,\mathbf{C}\,\mathbf{C}^t\left[\frac{d}{dx}\mathbf{P}(x)^t\right] = \mathbf{P}(x)\left[\frac{d}{dx}\mathbf{P}(x)^t\right] = \mathbf{P}(x)\left[\frac{d}{dx}\mathbf{P}(x)\right]^t\end{aligned} \tag{41}$$

where we have used identities $\mathbf{C}\,\mathbf{C}^t = \mathbf{I}$ and $\frac{d}{dx}\mathbf{C} = \mathbf{0}$.
Considering the structure (26) of $\mathbf{P}(x)$, the product $\mathbf{P}(x)\left[\frac{d}{dx}\mathbf{P}(x)\right]^t$ can be expanded as:

$$\mathbf{P}(x)\left[\frac{d}{dx}\mathbf{P}(x)\right]^t = \left(\begin{array}{cc|cc|cc|c} 0 & -1 & 0 & 0 & 0 & 0 & \\ 1 & 0 & 0 & 0 & 0 & 0 & \\ \hline 0 & 0 & 0 & -3 & 0 & 0 & \\ 0 & 0 & 3 & 0 & 0 & 0 & \\ \hline 0 & 0 & 0 & 0 & 0 & -5 & \\ 0 & 0 & 0 & 0 & 5 & 0 & \\ \hline & & & & & & \ddots \end{array}\right) = \mathbf{J} \tag{42}$$

The final expression for the machine voltage equation in orthonormal coordinates is then:

$$\mathbf{v}_{dq} = \mathbf{R}_{dq}\mathbf{i}_{dq} + \omega\mathbf{J}\mathbf{L}_{dq}\mathbf{i}_{dq} + \mathbf{L}_{dq}\frac{d}{dt}\mathbf{i}_{dq} + \mathbf{e}_{dq} \tag{43}$$

which is formally identical to the transformed voltage equation of a three-phase synchronous machine in the rotor dq reference frame.
From (44) a simple expression for the machine electromagnetic torque can be also derived. In fact, if we left-multiply both sides of (44) by $\mathbf{i}_{dq}{}^t$ we obtain:

$$\mathbf{i}_{dq}{}^t\mathbf{v}_{dq} = \mathbf{i}_{dq}{}^t\mathbf{R}_{dq}\mathbf{i}_{dq} + \omega\mathbf{i}_{dq}{}^t\mathbf{J}\mathbf{L}_{dq}\mathbf{i}_{dq} + \mathbf{i}_{dq}{}^t\mathbf{L}_{dq}\frac{d}{dt}\mathbf{i}_{dq} + \mathbf{i}_{dq}{}^t\mathbf{e}_{dq}\,. \tag{44}$$

Using (10), (11), (24), we can write the left-hand side member of (45) as follows:

$$\mathbf{i}_{dq}{}^t\mathbf{v}_{dq} = \left[\mathbf{T}(x)\mathbf{i}_s\right]^t\mathbf{T}(x)\mathbf{v}_s = \mathbf{i}_s{}^t\mathbf{T}(x)^t\mathbf{T}(x)\mathbf{v}_s = \mathbf{i}_s{}^t\mathbf{v}_s = \sum_{k=0}^{n-1} v_k i_k = p_e \tag{45}$$

where p_e is the instantaneous electrical power entering machine terminals; using (14) and (28), the term $\mathbf{i}_{dq}{}^t\mathbf{R}_{dq}\mathbf{i}_{dq}$ can be written as:

$$\mathbf{i}_{dq}{}^t\mathbf{R}_{dq}\mathbf{i}_{dq}{}^t = r\,\mathbf{i}_{dq}{}^t\mathbf{i}_{dq}{}^t = \sum_{k=0}^{n-1} r i_k{}^2 = p_j \tag{46}$$

where p_j is the total amount of joule losses in stator phases; finally, the term $\mathbf{i}_{dq}{}^t\mathbf{L}_{dq}\frac{d}{dt}\mathbf{i}_{dq}$ can be written as:

$$\mathbf{i}_{dq}{}^t\mathbf{L}_{dq}\frac{d}{dt}\mathbf{i}_{dq}=\frac{d}{dt}w_{mag}=\frac{d}{dt}\left(\frac{1}{2}\mathbf{i}_{dq}{}^t\mathbf{L}_{dq}\mathbf{i}_{dq}\right)=p_{mag} \tag{47}$$

where p_{mag} is the amount of power used to change the magnetic energy $w_{mag}=\frac{1}{2}\mathbf{i}_{dq}{}^t\mathbf{L}_{dq}\mathbf{i}_{dq}$ stored in machine magnetic circuits. As a result of (46)-(48), equation (45) becomes:

$$p_e=p_j+p_{mag}+p_m\,. \tag{48}$$

where

$$p_m=\omega\mathbf{i}_{dq}{}^t\mathbf{J}\mathbf{L}_{dq}\mathbf{i}_{dq}+\mathbf{i}_{dq}{}^t\mathbf{e}_{dq}\,. \tag{49}$$

is the part of the power converted into mechanical power. Then, the power p_m can be also written in terms of electromagnetic machine torque T_{em} and mechanical rotor speed ω_m:

$$p_m=T_{em}\,\omega_m=T_{em}\frac{\omega}{p}\,. \tag{50}$$

where p is the number of pole pairs. By equalling (50) and (51) one obtains the expression for the electromagnetic torque:

$$T_{em}=p\,\mathbf{i}_{dq}{}^t\mathbf{J}\mathbf{L}_{dq}\mathbf{i}_{dq}+\frac{p}{\omega}\mathbf{i}_{dq}{}^t\mathbf{e}_{dq} \tag{51}$$

where the first term represents the reluctance torque component (due to rotor saliency and acting even in absence of rotor MMF) and the second term represents the torque component due to the interaction between stator and rotor magneto-motive force fields.
The electromagnetic torque (52) is to be used along with the externally-applied torque T_{ext} in the mechanical differential equation which governs the shaft speed dynamics:

$$T_{em}-T_{ext}=J\frac{d\omega_m}{dt}+B\omega_m \tag{52}$$

where J is the rotor moment of inertia, B is the viscous friction coefficient and ω_m is mechanical rotor speed, equal to ω/p.

4. VSD model implementation in the Matlab/Simulink environment

The mathematical modelling of the multiphase machines described above is suitable for a modular, scalable and flexible implementation in the Matlab/Simulink environment.
A block scheme which can be used for this purpose is provided in Fig. 8, where the particular case of a multiphase synchronous machine with wound-field rotor is considered. Of course, the same scheme holds in case of induction machines as well as for Permanent Magnet (PM) or reluctance synchronous machines, provided that the field voltage input is removed or properly replaced.

The overall system comprises a "Simulink domain", where the multiphase machine model is implemented, and a "SimPowerSystems domain" where the power electronics connected to the machine is modelled.

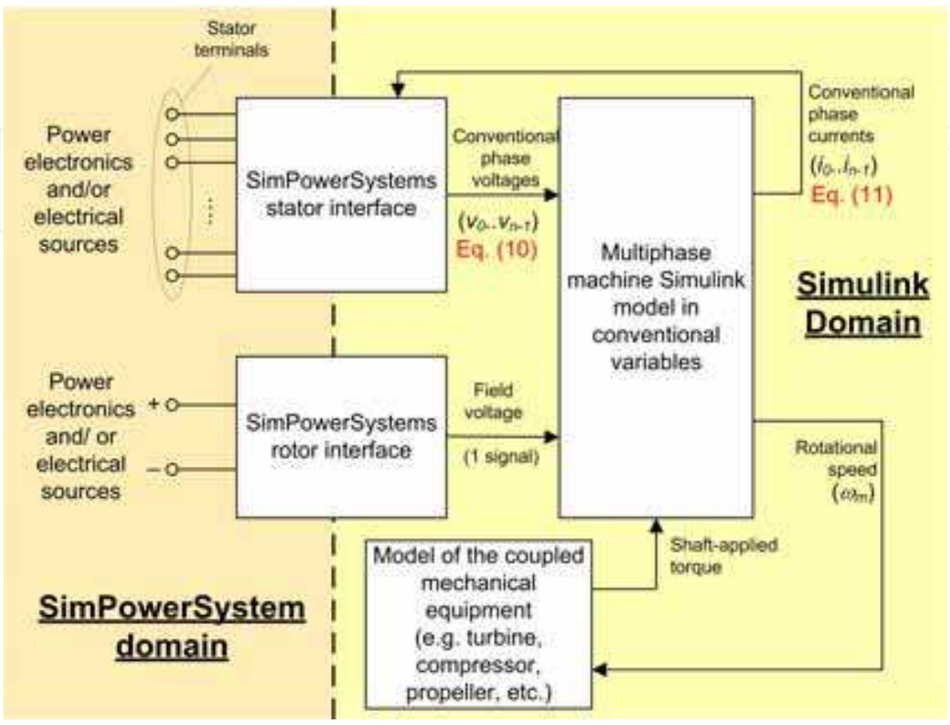

Fig. 8. Block scheme of the Simulink implementation of the multiphase machine model

4.1 Implementation of multiphase machine model in conventional phase variables

The core of the system represented in Fig. 8 is constituted by the "Multiphase machine Simulink model in conventional variables" block, whose detailed structure is depicted in Fig. 9. It implements the differential equations of the machine under the hypothesis that stator phases are geometrically arranged according to the "conventional" n-phase scheme discussed in 3.1. Therefore, the mathematical model implemented is the one described in Section 3.2 of this Chapter. The choice of using conventional variables makes the block independent of the phase arrangement and on the phase number.

In order to be implemented using phase currents as state variables, the stator voltage equation (44) is rewritten in the following form:

$$\frac{d}{dt}\mathbf{i}_{dq} = -\mathbf{L}_{dq}^{-1}\left(\mathbf{R}_{dq} + \omega\mathbf{J}\mathbf{L}_{dq}\right)\mathbf{i}_{dq} + \mathbf{L}_{dq}^{-1}\left(\mathbf{v}_{dq} - \mathbf{e}_{dq}\right) \tag{53}$$

This differential equation directly maps into the block scheme shown in Fig. 9.

As to the torque equation, it is implemented according to (52) as it does not involve any dynamics. Finally, the mechanical equation (53) is rewritten for implementation as:

$$\frac{d\omega_m}{dt} = \frac{1}{J}\left(T_{em} - T_{ext}\right) - \frac{B}{J}\omega_m \tag{54}$$

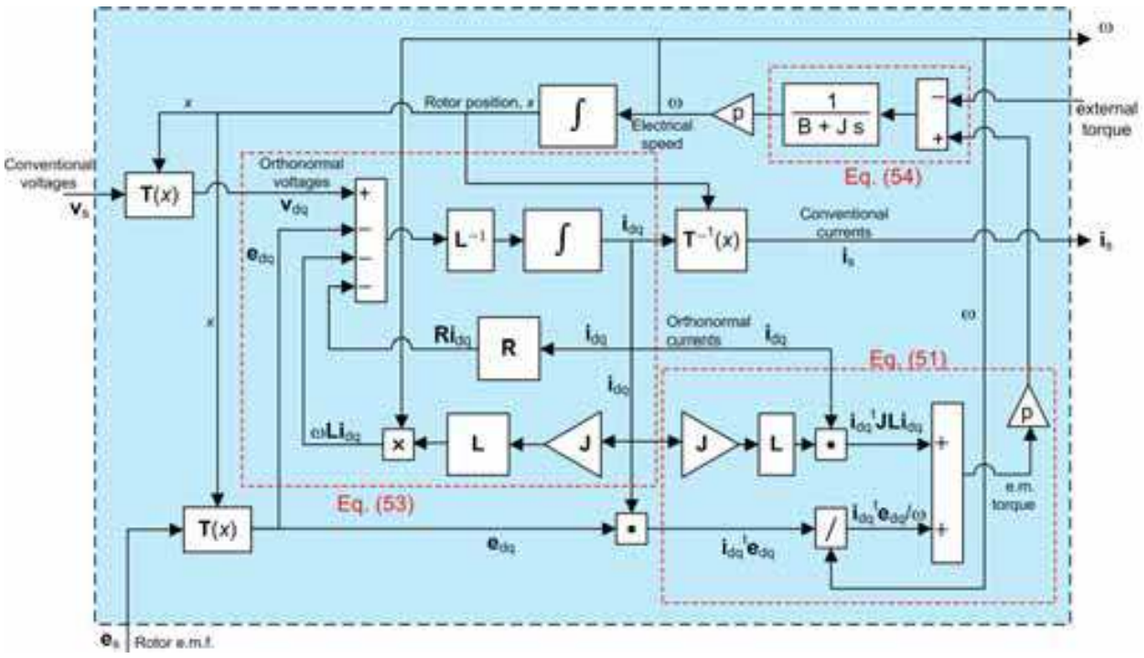

Fig. 9. Internal structure of the model "Multiphase machine Simulink model in conventional variables"

Beside implementing equations (52), (54) and (55), the block scheme in Fig. 4 includes the variable transformation $\mathbf{T}(x)$, defined by (25)-(27), between the conventional multiphase variable vectors (10)-(11) and the orthonormal coordinate vectors (24).

4.2 Interface with external blocks

The machine block shown in Fig. 9 accepts "conventional voltages" $\mathbf{v}_s$ as inputs and provides "conventional currents" $\mathbf{i}_s$ as outputs. The actual machine phases, however, are not arranged according to the conventional multiphase scheme assumed for unification purposes as per 3.1. Therefore, for the machine block to communicate with external blocks, it is necessary to "reorder" or "permute" conventional variable vectors to obtain the vectors of the physical (or natural) phase voltages and currents.

Moreover, external blocks interfaced with the machine model are often representative of power electronics equipment since it is very unusual that a multiphase machine is directly connected to the grid or to passive loads. Power electronics blocks, used to simulate inverters or converters, are generally built using SimPowerSystems library items.

As a result, the "stator interface" block appearing in Fig. 8 is added to perform these two tasks (the internal block structure is shown in Fig. 10):

1. Machine variable transformation between "conventional" and "natural" coordinate systems.
2. Conversion of machine phase voltages and currents from plain Simulink signals into SimPowerSystems bus attributes.

The former task is performed by means of the permutation matrices $\mathbf{W}$ introduced in 3.1 and 3.2.

The latter task is performed making use of one ideal current generator block and one voltage measurement block per machine phase. More precisely, the voltage across each

machine phase is measured and used to build the natural phase voltage vector, which will be then transformed into the conventional phase voltage vector through matrix **W**. The natural phase currents which come from the machine model, instead, are imposed to flow across their relative phase bus by means of the ideal current generators.

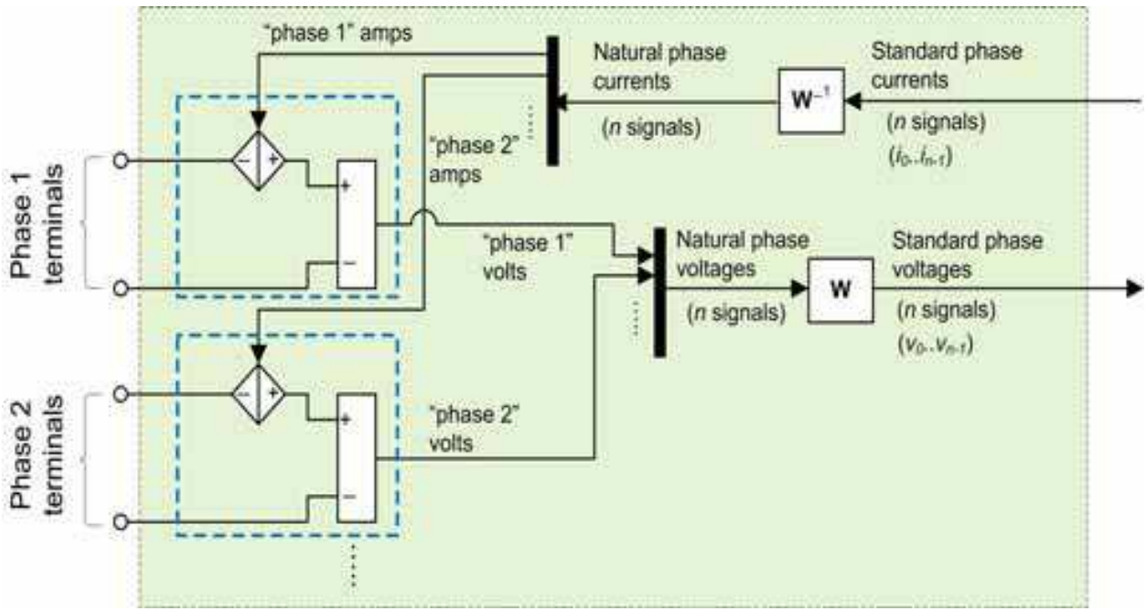

Fig. 10. Internal structure of the stator interface block

4.3 Model parameterization, initialization and adaptation to different multiphase machines

The advantage of the multiphase machine model implementation presented in this Chapter is that it can be easily parametrized and initialized so as to adapt it to simulate various kinds of multiphase machines, differing by the number and geometrical arrangement of the phases.

4.3.1 Parametrization

The input parameters which the user has to define, as far as the stator portion of the model is concerned, are the following:

a. The number of phases
b. The phase arrangement, to be chosen among the types described in Section 2. Typically: *n*-phase symmetrical or asymmetrical, in the latter case specifying the number *N* of winding sections and the number *m* of phases per section.
c. The phase resistance *r*, to be used to build the diagonal resistance matrix **R** as per (28).
d. The phase harmonic inductances (31), to build the diagonal transformed inductance matrix (30).

4.3.2 Initialization

The initialization can be performed through a Matlab script run only once at the beginning of the simulation. The script performs the following tasks:

a. It assigns the permutation matrices **W** in the stator interface blocks (Fig. 10). Permutation matrices are selected and defined as per 3.2.1 and 3.2.2 depending on the phase number and arrangement specified as an input;
b. It defines the variable transformation matrix **T**(x) as per (25) depending only on the number of phases;
c. It builds the diagonal matrices **R** and inductance matrix **L** using respectively the phase resistance and stator harmonic inductances (31) specified as input data;
d. It builds the constant block-diagonal matrix J as per (43) depending only on the number of stator phases.

4.3.3 Model adaptation to different multiphase winding schemes

The adaptation of the model to implement different winding schemes can be essentially done in the initialization stage simply by properly defining the various model matrices as the model structure essentially remains the same. Of course, for an n-phase machine, we shall have *n* pairs of terminals (one pair per phase) and thereby *n* of the blocks marked with blue dashed contour in Fig. 10.

5. Examples of application

To illustrate the possible application of the method described in this Chapter, we next report the case of a dual-star and a triple-star synchronous machines (the dual and triple three-phase winding schemes are respectively shown in Fig. 1b and in Fig. 5a). The former (2 MW, 1200 V, 6300 rpm) is operated as a motor fed by two Load-Commutated Inverters (Castellan et al., 2008), the latter (20 kVA, 720 V, 3000 V) is operated as a driven generator with its stator terminals in short circuit. Both machines are simulated using the same Matlab/Simulink model, described in Section 3, adapted to the two cases by a different initialization of its matrices [**W**, **C**, **P**(*x*)] as reported below.
Provided that natural phase variables are arranged in vector form as follows

$$\mathbf{y}_{2\times ABC} = \begin{pmatrix} y_{A1} & y_{A2} & y_{B1} & y_{B2} & y_{C1} & y_{C2} \end{pmatrix}^t, \tag{55}$$

$$\mathbf{y}_{3\times ABC} = \begin{pmatrix} y_{A1} & y_{B1} & y_{C1} & y_{A2} & y_{B2} & y_{C2} & y_{A3} & y_{B3} & y_{C3} \end{pmatrix}^t, \tag{56}$$

the permutation matrices in the two cases are given by (58) and (59) and the transformation matrices **C** and **P**(*x*), used to build **T**(*x*)=**P**(*x*)**C**, are given by (60)-(63).
The Matlab/Simulink models used for the simulations are shown in Fig. 11 and Fig. 12, where the yellow block represents the same model differently initialized to represent the two different machines (shown in Fig. 13).

$$\mathbf{W}_{2\times 3} = \begin{pmatrix} 1 & 0 & 0 & 0 & 0 & 0 \\ 0 & 0 & 0 & 1 & 0 & 0 \\ 0 & 0 & -1 & 0 & 0 & 0 \\ 0 & 0 & 0 & 0 & 0 & -1 \\ 0 & 1 & 0 & 0 & 0 & 0 \\ 0 & 0 & 0 & 0 & 1 & 0 \end{pmatrix}, \tag{57}$$

$$\mathbf{W}_{3\times3}=\begin{pmatrix}1&0&0&0&0&0&0&0&0\\0&0&0&1&0&0&0&0&0\\0&0&0&0&0&0&1&0&0\\0&0&-1&0&0&0&0&0&0\\0&0&0&0&0&-1&0&0&0\\0&0&0&0&0&0&0&0&-1\\0&1&0&0&0&0&0&0&0\\0&0&0&0&1&0&0&0&0\\0&0&0&0&0&0&0&1&0\end{pmatrix}', \tag{58}$$

$$\mathbf{C}_6=\sqrt{\frac{2}{6}}\begin{pmatrix}1&\cos(\alpha_6)&\cos(2\alpha_6)&\cos(3\alpha_6)&\cos(4\alpha_6)&\cos(5\alpha_6)\\0&\sin(\alpha_6)&\sin(2\alpha_6)&\sin(3\alpha_6)&\sin(4\alpha_6)&\sin(5\alpha_6)\\1&\cos(3\alpha_6)&\cos(6\alpha_6)&\cos(9\alpha_6)&\cos(12\alpha_6)&\cos(15\alpha_6)\\0&\sin(3\alpha_6)&\sin(6\alpha_6)&\sin(9\alpha_6)&\sin(12\alpha_6)&\sin(15\alpha_6)\\1&\cos(5\alpha_6)&\cos(10\alpha_6)&\cos(15\alpha_6)&\cos(20\alpha_6)&\cos(25\alpha_6)\\0&\sin(5\alpha_6)&\sin(10\alpha_6)&\sin(15\alpha_6)&\sin(20\alpha_6)&\sin(25\alpha_6)\end{pmatrix} \tag{59}$$

$$\mathbf{C}_9=\sqrt{\frac{2}{9}}\begin{pmatrix}1&\cos(\alpha_9)&\cos(2\alpha_9)&\cdots&\cos(8\alpha_9)&\cos(9\alpha_9)\\0&\sin(\alpha_9)&\sin(2\alpha_9)&\cdots&\sin(8\alpha_9)&\sin(9\alpha_9)\\1&\cos(3\alpha_9)&\cos(6\alpha_9)&\cdots&\cos(24\alpha_9)&\cos(27\alpha_9)\\0&\sin(3\alpha_9)&\sin(6\alpha_9)&\cdots&\sin(24\alpha_9)&\sin(27\alpha_9)\\1&\cos(5\alpha_9)&\cos(10\alpha_9)&\cdots&\cos(40\alpha_9)&\cos(45\alpha_9)\\0&\sin(5\alpha_9)&\sin(10\alpha_9)&\cdots&\sin(40\alpha_9)&\sin(45\alpha_9)\\1&\cos(7\alpha_9)&\cos(14\alpha_9)&\cdots&\cos(56\alpha_9)&\cos(63\alpha_9)\\0&\sin(7\alpha_9)&\sin(14\alpha_9)&\cdots&\sin(56\alpha_9)&\sin(63\alpha_9)\\\frac{1}{\sqrt{2}}&\frac{1}{\sqrt{2}}\cos(9\alpha_9)&\frac{1}{\sqrt{2}}\cos(18\alpha_9)&&\frac{1}{\sqrt{2}}\cos(72\alpha_9)&\frac{1}{\sqrt{2}}\cos(81\alpha_9)\end{pmatrix} \tag{60}$$

$$\mathbf{P}_6(x)=\begin{pmatrix}\cos(x)&\sin(x)&0&0&0&0\\-\sin(x)&\cos(x)&0&0&0&0\\0&0&\cos(3x)&\sin(3x)&0&0\\0&0&-\sin(3x)&\cos(3x)&0&0\\0&0&0&0&\cos(5x)&\sin(5x)\\0&0&0&0&-\sin(5x)&\cos(5x)\end{pmatrix} \tag{61}$$

$$\mathbf{P}_9(x)=\begin{pmatrix}\cos(x)&\sin(x)&0&0&0&0&0&0&0\\-\sin(x)&\cos(x)&0&0&0&0&0&0&0\\0&0&\cos(3x)&\sin(3x)&0&0&0&0&0\\0&0&-\sin(3x)&\cos(3x)&0&0&0&0&0\\0&0&0&0&\cos(5x)&\sin(5x)&0&0&0\\0&0&0&0&-\sin(5x)&\cos(5x)&0&0&0\\0&0&0&0&0&0&\cos(7x)&\sin(7x)&0\\0&0&0&0&0&0&-\sin(7x)&\cos(7x)&0\\0&0&0&0&0&0&0&0&1\end{pmatrix} \tag{62}$$

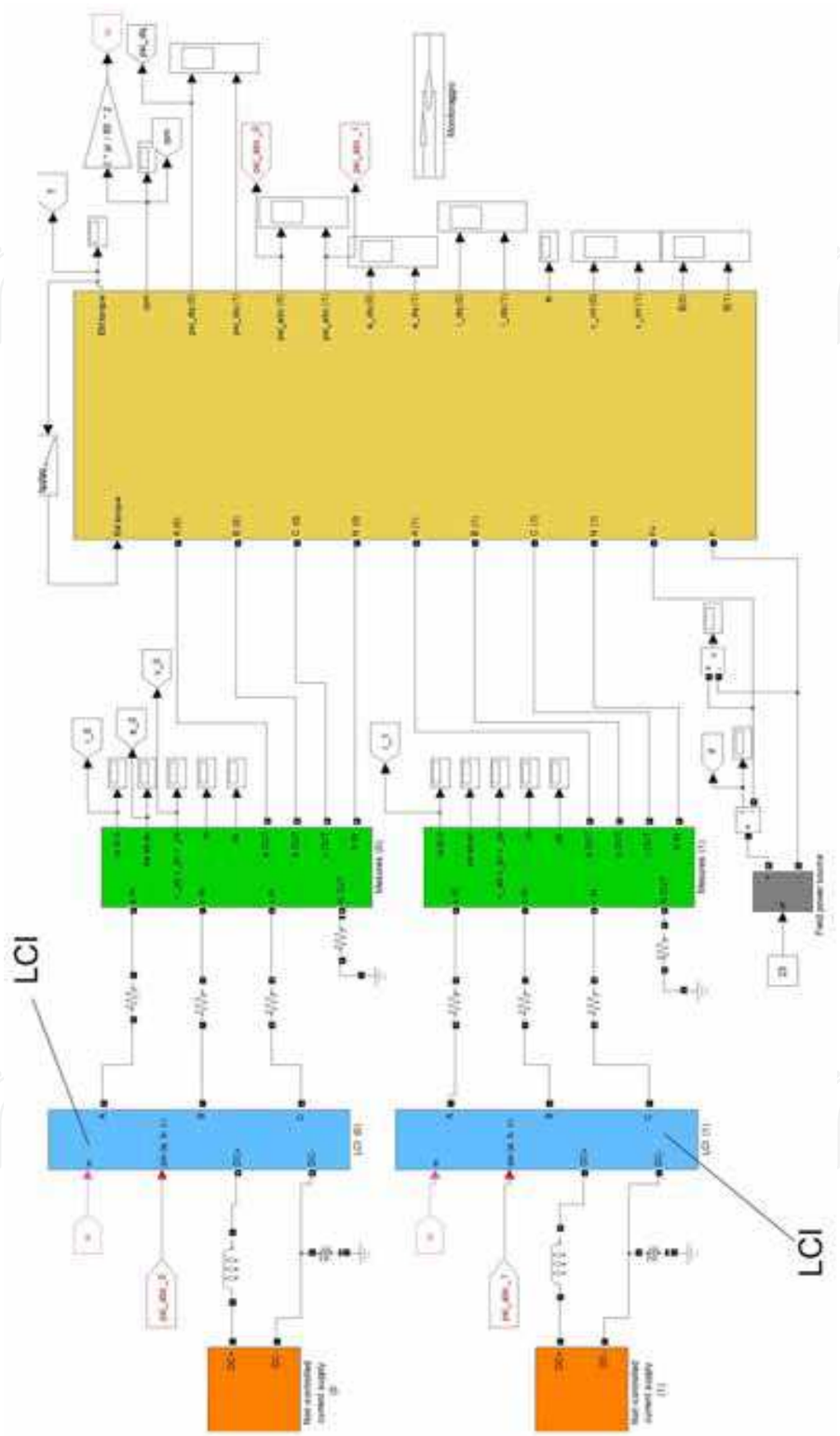

Fig. 11. Matlab/Simulink model for the simulation of a dual-star synchronous machine supplied by two Load-Commutated Inverters

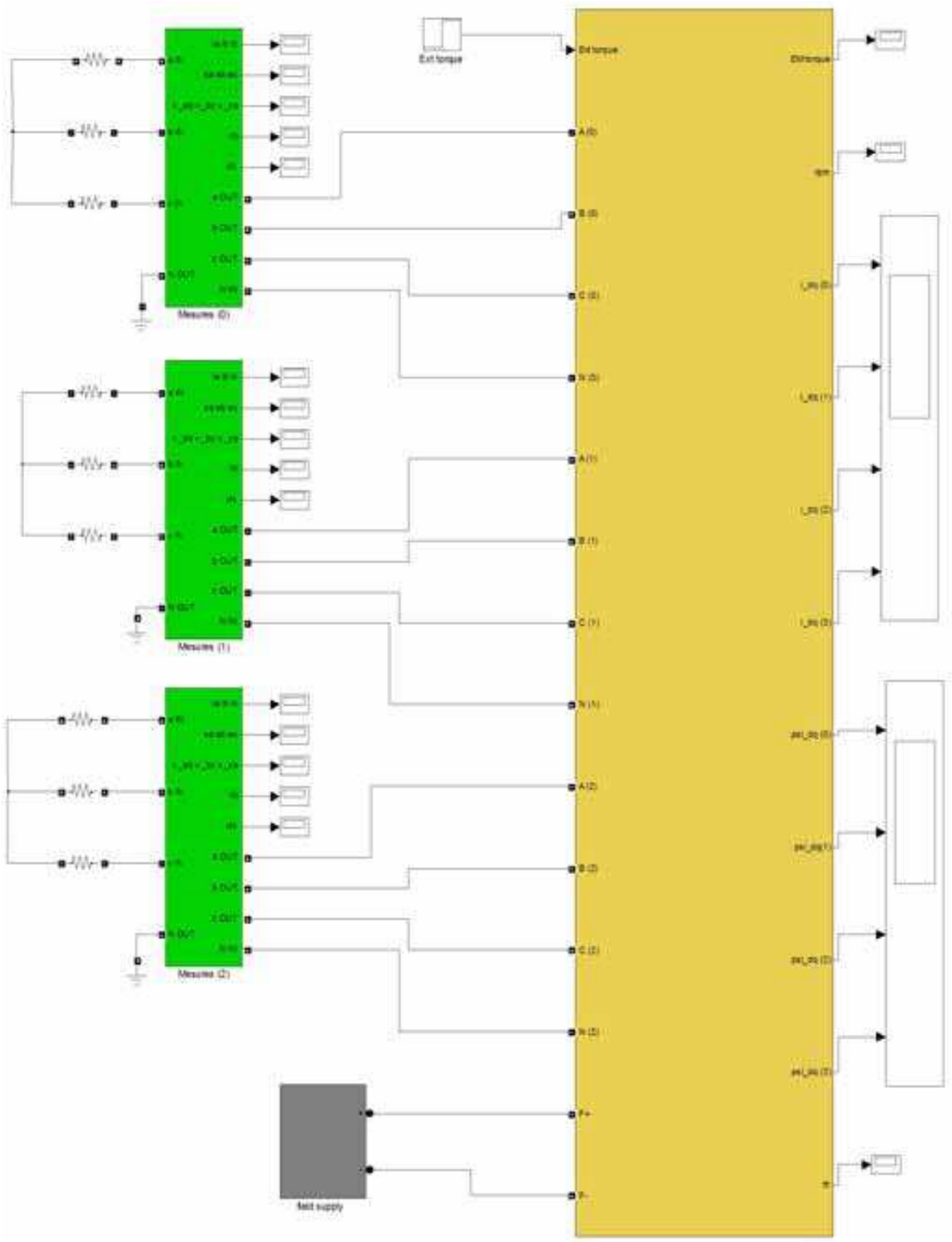

Fig. 12. Matlab/Simulink model for the simulation of a triple-star synchronous machine operating as a driven generator with short-circuited stator terminals

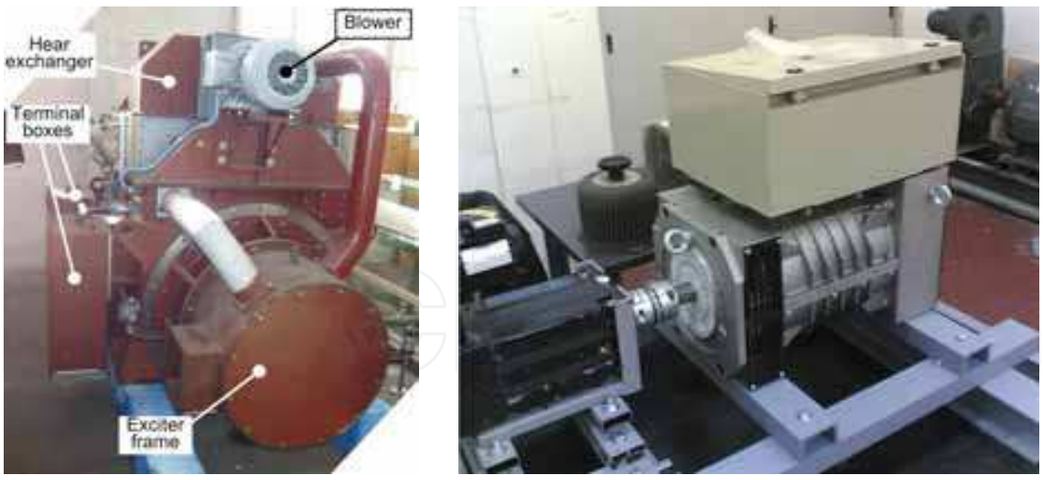

(a) (b)

Fig. 13. (a) Dual-star synchronous motor (2 MW, 1200V, 6300 rpm) to be fed from two LCIs. (b) Triple-star synchronous generator driven with short-circuit stator terminals

Simulation results, compared with measurements, for the dual- and triple-star machine are reported in Fig. 14 and Fig. 15, showing a good accordance in all the operating conditions

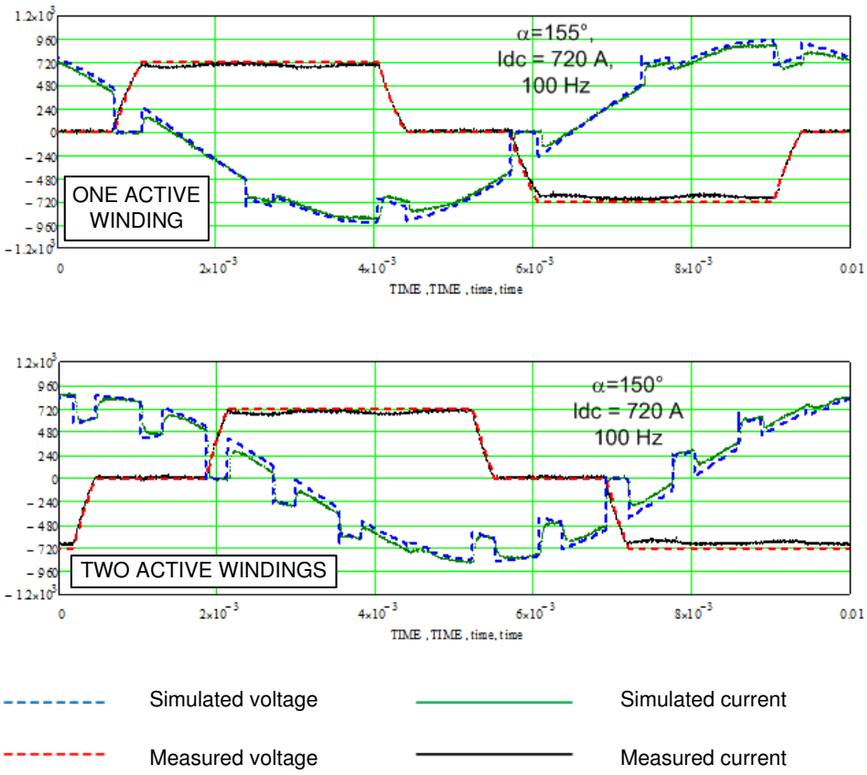

Fig. 14. Comparison between simulated and measured voltages and currents for the dual-star synchronous motor under LCI supply in case of both active windings and one single active winding

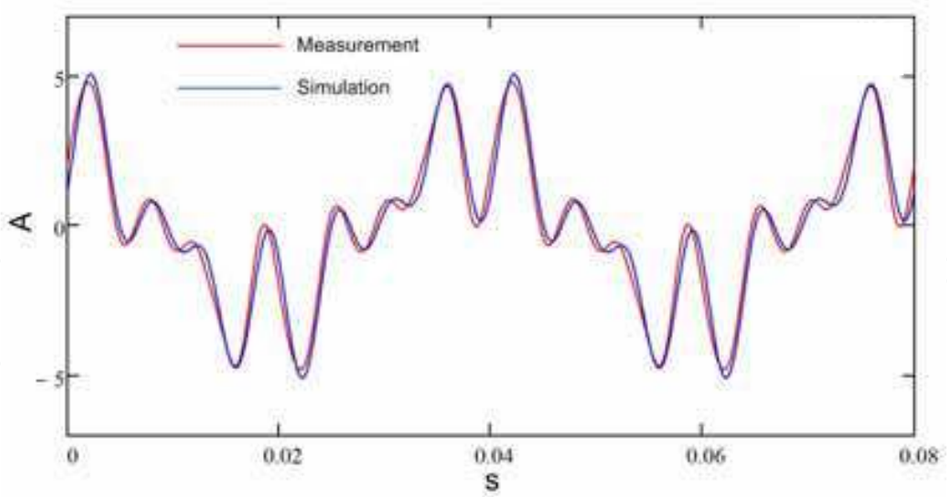

Fig. 15. Comparison between simulated and measured short-circuit current in a triple-star generator driven with short-circuited stator terminals

A further application examples of the methodology described in this Chapter can found in Tessarolo et al., 2009, where the same synchronous machine model used for the two simulation cases reported in this Section has been employed to simulate a symmetrical five-phase synchronous motor fed by a five-phase Load Commutated Inverter.

6. References

E. Levi, "Multiphase electric machines for variable-speed applications", IEEE Trans. on Industrial Electronics, vol. 55, May 2008, pp. 1893-1909.

E. Levi, R. Bojoi, F. Profumo, H.A. Tolyat, S. Williamson, "Multiphase induction motor drives – a technology status review", Electric Power Application, IET, 2007, July 2007, vol. 1, pp. 489-516.

A. Tessarolo, G. Zocco, C. Tonello, "Design and testing of a 45-MW 100-Hz quadruple-star synchronous motor for a liquefied natural gas turbo-compressor drive", International Symposium on Power Electronics, Electrical Drives, Automation and Motion, SPEEDAM 2010, 14-16 June 2010, Pisa, Italy, pp. 1754-1761.

S. Castellan, R. Menis, M. Pigani, G. Sulligoi, A. Tessarolo, "Modeling and simulation of electric propulsion systems for all-electric cruise liners", IEEE Electric Ship Technologies Symposium, IEEE ESTS 2007, 21-23 May 2007, Arlington, VA, USA, pp. 60-64.

G. Sulligoi, A. Tessarolo, V. Benucci, M. Baret, A. Rebora, A. Taffone, "Modeling, simulation and experimental validation of a generation system for Medium-Voltage DC Integrated Power Systems", IEEE Electric Ship Technologies Symposium, 2009, ESTS 2009, 20-22 April 2009, Baltimora, US, pp. 129- 134.

S. Castellan, G. Sulligoi, A. Tessarolo, "Comparative performance analysis of VSI-fed and CSI-fed supply solutions for high power multi-phase synchronous motor drives", International Symposium on Power Electronics, Electrical Drives, Automation and Motion, SPEEDAM 2008, 11-13 June 2008, Ischia, Italy, pp. 854-859.

L.A. Pereira, C. C. Scharlau, L.F.A. Pereira, J.F. Haffner, "General model of a five-phase induction machine allowing for harmonics in the air-gap", *IEEE Trans. on Energy Conversion*, vol. 21, issue 4, Dec. 2006, pp. 891-899.

J. Figueroa, J. Cros, P. Viarouge, "Generalized Transformations for Polyphase Phase-Modulated Motors", *IEEE Transactions On Energy Conversion*, vol. 21, June 2006, pp. 332-341.

F. Terrein, S. Siala, P. Noy, "Multiphase induction motor sensorless control for electric ship propulsion", *IEE Power Electronics, Machines and Drives Conference*, PEMD 2004, pp. 556-561.

E.A. Klingshirn, "High phase order induction motors–Part I–Description and theoretical considerations", *IEEE Trans. on Power Apparatus and Systems*, Jan. 1983, vol. PAS-102, pp. 47-53.

A. Tessarolo, "On the modeling of poly-phase electric machines through Vector-Space Decomposition: theoretical considerations", *International Conference on Power Engineering, Energy and Electrical Drives*, *POWERENG 2009*, 18-20 March 2009, Lisbon, Portugal, 18-20 March 2009, pp. 519-523.

A. Tessarolo, S. Castellan, R. Menis, "Analysis and simulation of a novel Load-Commutated Inverter drive based on a five-phase synchronous motor", *European Conference on Power Electronics and Applications, 2009, EPE '09*, 8-10 Sept. 2009, Barcelona, Spain, CD-ROM paper.

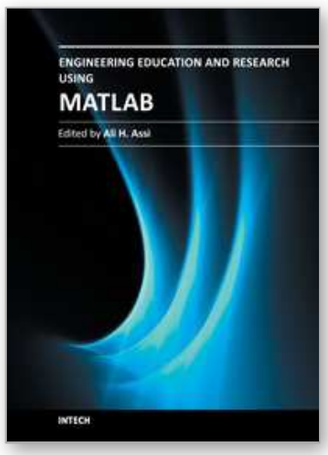

Engineering Education and Research Using MATLAB

Edited by Dr. Ali Assi

ISBN 978-953-307-656-0

Hard cover, 480 pages

Publisher InTech

Published online 10, October, 2011

Published in print edition October, 2011

MATLAB is a software package used primarily in the field of engineering for signal processing, numerical data analysis, modeling, programming, simulation, and computer graphic visualization. In the last few years, it has become widely accepted as an efficient tool, and, therefore, its use has significantly increased in scientific communities and academic institutions. This book consists of 20 chapters presenting research works using MATLAB tools. Chapters include techniques for programming and developing Graphical User Interfaces (GUIs), dynamic systems, electric machines, signal and image processing, power electronics, mixed signal circuits, genetic programming, digital watermarking, control systems, time-series regression modeling, and artificial neural networks.

INTECH

open science | open minds

InTech Europe

University Campus STeP Ri
Slavka Krautzeka 83/A
51000 Rijeka, Croatia
Phone: +385 (51) 770 447
Fax: +385 (51) 686 166
www.intechopen.com

InTech China

Unit 405, Office Block, Hotel Equatorial Shanghai
No.65, Yan An Road (West), Shanghai, 200040, China
中国上海市延安西路65号上海国际贵都大饭店办公楼405单元
Phone: +86-21-62489820
Fax: +86-21-62489821

IntechOpen